Ultrasonic wave propagation in heterogeneous media

Laura Cunningham, Anthony Mulholland, Gerald Harvey, Colin Bird

▶ **To cite this version:**

Laura Cunningham, Anthony Mulholland, Gerald Harvey, Colin Bird. Ultrasonic wave propagation in heterogeneous media. Acoustics 2012, Apr 2012, Nantes, France. hal-00810926

HAL Id: hal-00810926
https://hal.science/hal-00810926

Submitted on 23 Apr 2012

HAL is a multi-disciplinary open access archive for the deposit and dissemination of scientific research documents, whether they are published or not. The documents may come from teaching and research institutions in France or abroad, or from public or private research centers.

L'archive ouverte pluridisciplinaire **HAL**, est destinée au dépôt et à la diffusion de documents scientifiques de niveau recherche, publiés ou non, émanant des établissements d'enseignement et de recherche français ou étrangers, des laboratoires publics ou privés.

ACOUSTICS 2012

Ultrasonic wave propagation in heterogeneous media

L. Cunningham[a], A. J. Mulholland[a], G. Harvey[b] and C. Bird[c]

[a]University of Strathclyde, Department of Mathematics and Statistics, 26 Richmond Street, G1 1XH Glasgow, UK
[b]PZFlex Europe, 50 Richmond Street, G1 1XP Glasgow, UK
[c]Doosan Babcock, T&E Building, Porterfield Rd, PA4 8DJ Renfrew, UK
laura.cunningham@strath.ac.uk

The non-destructive testing of austenitic steel welds using ultrasound is of vital importance for assessing safety critical structures such as those found in the nuclear industry. The internal geometry of these welds is heterogeneous and highly scattering and this makes it difficult to detect and characterise any defects within them. To help overcome these difficulties the use of ultrasound transducer arrays and the associated Full Matrix Capture is becoming more widespread. There is a need therefore to develop post-processing algorithms that best utilise the data from such devices. This paper considers the use of a time-frequency domain method known as the Decomposition of the Time Reversal Operator (DORT) method. To develop this method and to demonstrate its efficacy in tackling this problem a series of simulated data sets are used. The simulated data is generated using a finite element method (PZFLEX) with the heterogeneous internal microstructure of the weld being given by previous Electron Backscatter Diffraction measurements. A range of artificial flaws are then inserted into this geometry. By varying the flaw size and type a comparison is conducted between the DORT method and the Total Focusing Method (TFM) and their relative ability to perform flaw detection assessed. Importantly, however, the DORT method relies on a Singular Value Decomposition in time and frequency space and this spectral information contains information about the flaw size and shape.

1 Introduction

Ultrasonic Non-Destructive Evaluation (NDE) procedures are used extensively across many industries and are vital in ensuring reliable operation of safety critical infrastructures [1, 2]. The detection of defects in these structures is critical, as early detection allows timely maintenance of any faults which can then prevent further damage or failure. In the energy sector one of the most important and ubiquitous materials is stainless steel, but this can be difficult to inspect due to its the heterogeneous nature. In particular, stainless steel welds are notoriously difficult to inspect using ultrasonic techniques.

Ultrasonic phased array systems have been used for many years in medical ultrasonics [3] and advances in transducer design has expanded the use of these systems into NDE. A phased array transducer [4] is made up of many piezoelectric elements which act as transmitters and receivers. These systems are capable of storing Full Matrix Capture data (FMC) and can cover a wider inspection area than traditional, single element transducers.

The increased use of ultrasonic arrays in NDE stimulated the development of imaging techniques which utilise the FMC data. Much of this work has been aimed at accurate focusing through heterogeneous materials. One powerful technique is the Time Reversal Mirror (TRM) [5, 6, 7], which is effective even if there are inhomogeneities between the transducer and the target. This method takes the recorded signals from one firing of the transducer and reverses the time delays (last-in first-out technique). These time delays are used to fire the transducer again focusing the energy on the scatterer. The Total Focusing Method (TFM) is probably the most widely used imaging technique which uses FMC data. It is based on using time delays to focus the ultrasonic waves at every point in the image domain [8]. A recent method, which extends time reversal techniques to the time and frequency domain, is the DORT method (French acronym for the decomposition of the time reversal operator) [9, 10].

The aim of this paper is to compare the performance of the DORT and TFM methods as image based, flaw detection techniques. In particular, these methods will be applied to simulated FMC data from an austenitic steel weld. The simulated data was generated using a finite element method (PZFlex) [11].The heterogeneous internal microstructure was obtained previously by Electron Backscatter Diffraction measurements [12, 13] and simulations which use this microstructure are presented in this paper. In addition, a side drilled hole flaw is inserted into this geometry to mimic the standard experimental setting.

2 Simulated data using PZFlex

In order to develop methods for the non-destructive detection and characterisation of weld defects using ultrasound transducer arrays it would be useful to have a large library of data sets arising from a broad range of flaw types, size, positions, and so forth. The manufacture of even one such test piece is very expensive and time consuming and so there is an opportunity for computer simulations of such experiments to play a vital role. In order to run such simulations it is imperative to have knowledge of the internal microstructure of these welds as the heterogeneous nature of the material has a marked effect on the passage of elastic energy through it. To begin with it is important to have one experimental test piece that can be fully characterised in this way. This test piece can then be used to validate the computer simulation by comparing experimental and simulated data. This should always be done prior to these simulations being expanded to incorporate a range of different flaws. Fortunately considerable effort has already been expended in this direction and a fully characterised austenitic steel weld has been achieved using Electron Backscatter Diffraction (EBSD) [12]. The resulting spatial resolution within the sample was of the order of 40 μm for a 67 mm thick weld. The internal microstructure that is produced consists of a partitioning of the weld area into a large set of sub-regions, each one of which has a different crystal orientation. In order to attribute elastic stiffnesses to these regions a second experiment was necessary. Here a thin slice of the material was taken and a series of through-transmission ultrasonic velocity calculations performed on each of the different sub-regions. Having acquired this information on the internal microstructure of the weld this was fed into the (explicit time-domain) finite element package PZFlex [11]. The simulation placed a 64 element ultrasonic array directly above the weld microstructure. The width of each element was 1.5 mm and the pitch (period) of the array was 2mm resulting in a total array length (aperture) of 128 mm. A 1.5 Mhz single sinusoid tone burst was trans-

mitted by one element and the time domain received echo recorded by all 64 elements. The particular transmitting element was then systematically changed by moving along the array until the full matrix of time domain data was captured. A small circular flaw was then inserted into the simulation. This flaw simulates the side drilled hole scenario often employed in experimental settings and as such its internal material properties are those of air. The size and location of this flaw, and indeed the degree of heterogeneity within the microstructure and the size and location of the grain structure, can all now be varied to create the desired library of data from these test samples. In section 3, consideration of how this data can be treated to recover the flaw position and size is discussed.

3 Post Processing Algorithms

The simulated data is provided in Full Matrix Capture (FMC) form. The FMC data is a three dimensional matrix, **H**, which records the time-domain ultrasound signal from each transmit receive pair in the ultrasonic array. It has dimension $N_{rx} \times N_{tx} \times N_t$, where N_{tx}, N_{rx} correspond to the number of array elements (receiving rx, transmitting tx) and N_t is the total number of discrete times. This is the full set of time-domain responses from an array and provides the maximum volume of data which can be used for post processing. A typical signal from one element of **H** is shown in Figure 1. This figure shows a typical signal received by the transducer for one tx-rx pair, it shows the amplitudes received against time. The first peak in the signal, labelled 'INITIAL RESPONSE', is the signal travelling across the transducer from the transmitting element to the receiving element. The second peak, which is labelled as 'FLAW', is the amplitude response from the signal encountering the flaw and the final peak, labelled 'BACKWALL', is the the response due to the signal encountering the backwall of the weld. The imaging algorithms discussed in Section 3.1 are used as methods for the detection of flaws and aim to isolate the part of the signal corresponding to the flaw.

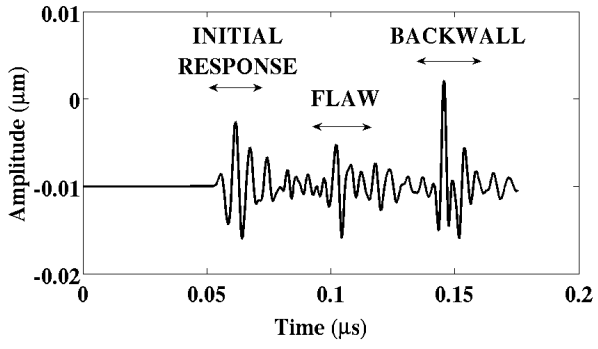

Figure 1: A typical signal from a weld including a 3.5mm diameter side drilled hole for one transmit-receive pair

3.1 The Total Focusing Method (TFM)

The Total Focusing Method (TFM) [8] is an imaging technique which exploits FMC data and can be used for the detection of defects in NDT. The TFM algorithm first requires the image domain to be discretized into a grid of pixels, $(N_x \times N_z)$. For each pixel, the signal from each transmit-receive (tx-rx) pair is focused at that point. The focusing is achieved by calculating the time of travel between a tx-rx pair and a fixed pixel (x, z), then using this to isolate the corresponding amplitude of the signal $\mathbf{H}(tx, rx, t)$. These amplitudes are then summed for each tx-rx pair and create the intensity for the pixel (x, z) in the image which is given by

$$I(x,z) = \left| \sum_{tx,rx} \mathbf{H}(tx, rx, t) \right| \tag{1}$$

where

$$t = \frac{\left(\sqrt{(x_{tx} - x)^2 + z^2} + \sqrt{(x_{rx} - x)^2 + z^2} \right)}{c_1} \tag{2}$$

and c_1 is the (usually longitudinal) speed of sound in the material, x_{rx} is the x-coordinate of the receiving element and x_{tx} is the x-coordinate of the transmitting element. In this scheme, the array is located at $z = 0$ and so $z_{tx} = z_{rx} = 0$.

This method is computationally very efficient for detection of flaws in isotropic materials. However, when the material is heterogenous, scattering of the ultrasonic waves occurs. There is no longer a direct path between a tx-rx pair and the flaw, and so the time delay calculations in Eq. (2) are no longer accurate.

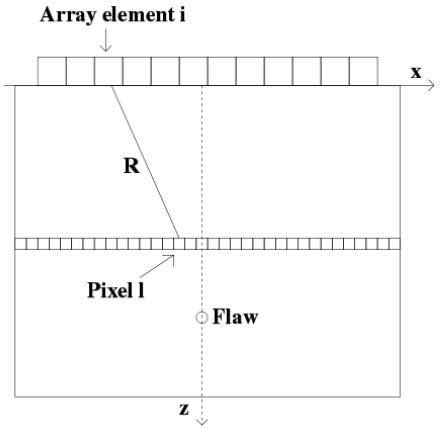

Figure 2: Geometry for back propagation, where $\mathbf{R} = r_{il}$ in Eq. (6)

3.2 The DORT Method

The DORT method [9] is an image processing method that uses time reversal techniques in the time-frequency domain, along with the singular value decomposition of the FMC data, to produce an image. The inter-element response matrix **K** is obtained by taking the time windowed discrete Fourier transform (DFT) of the FMC data, **H**. For each fixed time T and time window $\triangle t$ the Fourier transform is taken over the window $[T - \triangle t, T + \triangle t]$. This forms the full set of response matrices $\mathbf{K}(T, f)$, which is an N_{rx}xN_{tx}xN_FxN_t matrix where N_F is the number of discrete frequencies.

The second stage in the DORT method is to determine the Singular Value Decomposition (SVD) of each response matrix $\mathbf{K}(T, f)$ for each time, T, and frequency, f, pair. Within the DORT method the SVD is used as a tool for image reconstruction. The SVD of the each response matrix $\mathbf{K}(T, f)$

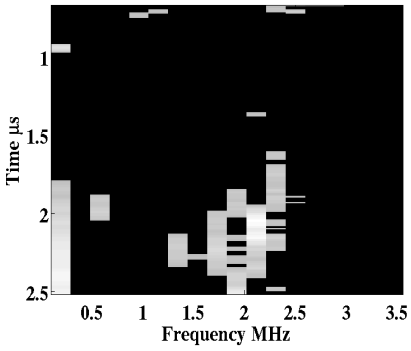

(a) r=0.25mm

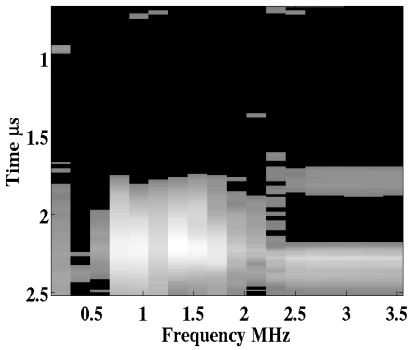

(b) r=1.25mm

Figure 3: First singular value distribution from the DORT method

is given by

$$\mathbf{K} = \mathbf{U}\Lambda\mathbf{V}^{\dagger} \tag{3}$$

where Λ is a diagonal matrix containing real, positive singular values λ_i, $i = 1, ..., N_{tx}$. For linear scatterers, each singular value is associated with one singular space. However, Chambers and Gautesen [14] have shown that there can be up to four singular values associated with one scattering event, and this number depends upon the shape and orientation of the scatterer. The left singular vector $\mathbf{V_1}$ provides information that can be used to focus the energy on the scatterer. Once the SVD of the data for each time-frequency pair, (T, f) is determined, the first singular values from each decomposition are normalized using their quadratic mean

$$\tilde{\lambda}_1(T, f) = \frac{\lambda_1(T, f)}{\sqrt{\frac{1}{N_{tx}} \sum_{p=1}^{N_{tx}} \lambda_p^2(T, f)}}. \tag{4}$$

By comparing this distribution to that found in a random matrix a detection threshold is applied to each $\tilde{\lambda}_1(T, f)$ [15].

Back propagation is then used to construct an image of the scatterer. The propagation operator is a Greens function, in the form of a 1 x N_x vector $\mathbf{G}$; the elements of which are given by

$$g_{il}(f) = \frac{\exp jkr_{il}}{\sqrt{r_{il}}} \tag{5}$$

where

$$r_{il} = \sqrt{z^2 + x_i^2}, \tag{6}$$

$z = cT/2$ is the depth in the material that is being imaged and x_i is the spatial position of array element i, as shown

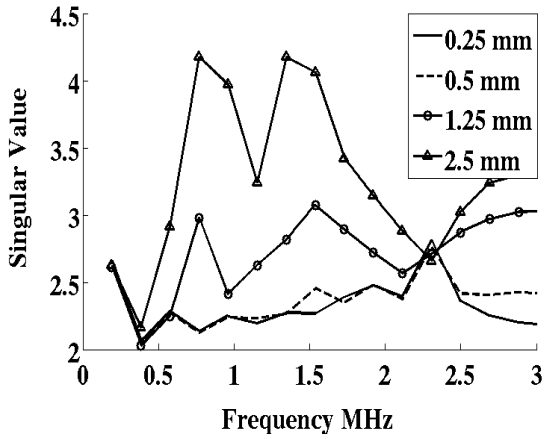

Figure 4: Frequency spectra of first singular value from simulated data with side drilled hole (SDH) inclusion of varying radius.

in Figure 2. Each point in the image, $I(T, x)$, is associated with the absolute value of the back propagated wave, which is focused using the first right eigenvector

$$I(T, x) = \sum_{f'} \lambda_1(T, f') |\mathbf{V_1}\mathbf{G}^*| \tag{7}$$

where f' corresponds to frequencies for which $\tilde{\lambda}_1(T, f)$ lies above the random matrix theory threshold and $\mathbf{G}^*$ is the complex conjugate of the Greens' function vector.

Table 1: Table of parameters used for the PZFlex simulations

Parameter	Value
Velocity	5808 m*extrms*$^{-}$1
δt	17.3 ns
Pitch	2 mm
Element width	1.5 mm
Number of elements	64
Radii of side drilled holes (mm)	0.25, 0.5, 0.75, 1, 1.25, 1.5, 1.75, 2, 2.5

4 Results

In this section we compare the peformance of the TFM and DORT methods discussed in Section **3**. These methods are applied to the simulated data produced using PZFlex (Section **2**). A range of these simulations are generated, each including a side drilled hole of varying radii (see Table 1). The side drilled hole is inserted in the centre of the weld at a depth of 50 mm. The ultrasonic array used is a 1.5MHz transducer, each array element is 1.5mm in size with a pitch of 2mm. A sample rate, δt, of 17.3 ns is used. These parameters are summarised in Table 1. For illustrative purposes the ultrasonic transducer is placed directly above the weld in this experimental configuration.

The DORT method is applied to the data sets described above. The first stage of the DORT method is to take the SVD of $\mathbf{K}$ for each time-frequency pair. For the data sets including side drilled holes of radius 0.25 mm and 1.25 mm, the first singular value distributions are illustrated in Figure

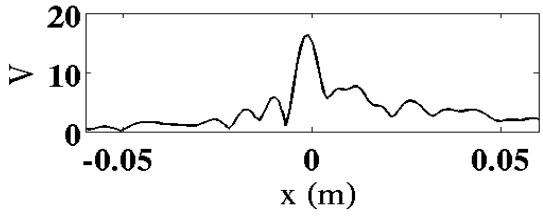

(a) V_1

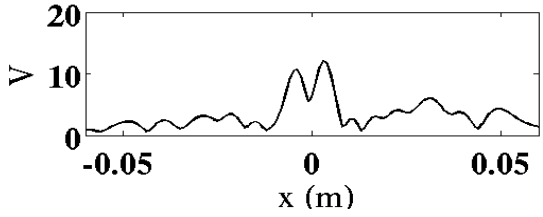

(b) V_2

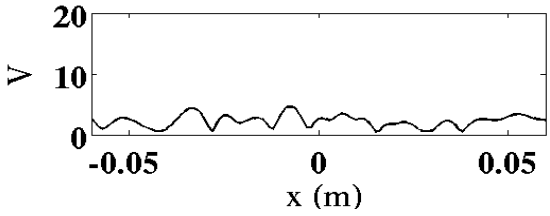

(c) V_3

Figure 5: Pressure plots of backpropagation of the right eigenvectors V_1, V_2 and V_3 with the Greens' function, where $\mathbf{V} = |\mathbf{V_i G}^*|$ with $i = 1, 2, 3$.

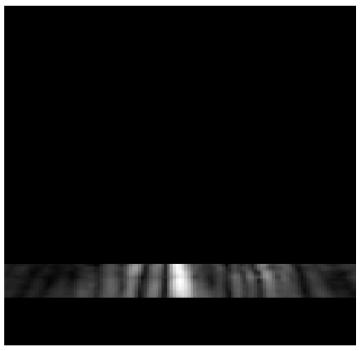

(a) r=0.25mm

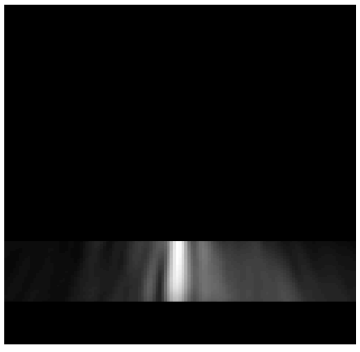

(b) r=1.25mm

Figure 6: Images of weld using the DORT method, r is the radius of the side drilled hole

3. This image shows $\tilde{\lambda_1}$ for each time-frequency pair in $\mathbf{K}$, the light grey and white areas indicate where $\tilde{\lambda_1}$ is above the

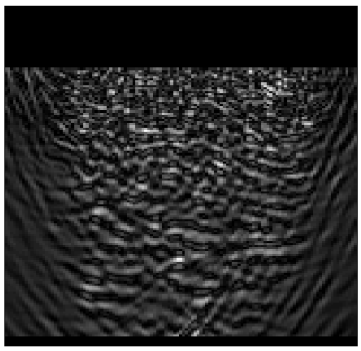

(a) r=0.25mm

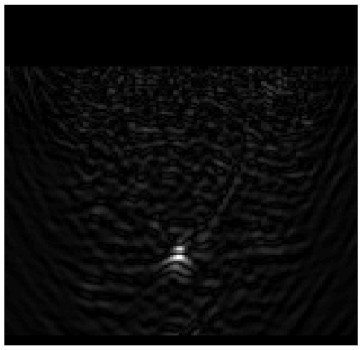

(b) r=1.25mm

Figure 7: Images of weld using the TFM method, r is the radius of the side drilled hole

detection threshold. These time-frequency pairs and corresponding singular values are used in the back propagation for the image reconstruction. It is clear from Figure 3 that there are more frequencies used in the image reconstruction of the weld including the larger side drilled hole. The frequency spectra of the first singular value, for welds including side drilled holes with radii 0.25 mm, 0.5 mm, 1.25 mm and 2.5 mm, is shown in Figure 4. This figure shows that as the size of the side drilled hole decreases the signature of the frequency spectra changes. The resonant peaks move to lower frequencies as one would anticipate from scattering theory [16]. An advantage of the DORT method is that it works in the time-frequency domain and the frequencies which are specific to the inclusion can be used to isolate data to use to create the image.

Pressure patterns of the back propagated waves using the first three right eigenvectors, V_1, V_2 and V_3, are shown in Figure 5. Using V_1 appears to produce the most focused wave with high energy in the centre of the array (which is directly above the flaw). This confirms that V_1 is the appropriate eigenvector to use for the focusing in the back propagation.

Figures 6 and 7 show the images produced when the DORT and TFM methods are applied to the simulated data including side drilled holes of radius 0.25 mm and 1.25 mm. The heterogenous nature of the weld microstructure can be seen in Figure 7b The DORT method only uses the data corresponding to the times where the first singular value is above the detection threshold (Figure 3) to create the image. Using this subsection of times means that an image is only produced at the depth of the flaw, as is shown in Figure 6. In Figure

7 the top section of the image is not filled, this is because this region contains the backscatter from the incident wave reflected in the near field. If this area were to be imaged, the high amplitudes would dominate here and other features, such as flaws, would not be visible. It can be seen from Figures 6a and 7a that when the radius of the side drilled hole is 0.25 mm the DORT method produces an image with a clearer detection of the flaw than the TFM method. However, in this experimental configuration the DORT method does not produce an image which clearly shows the size of the flaw, here it is used purely as a detection technique.

5 Conclusion

A comparison of the DORT and TFM methods as imaging processing tools for the detection of small defects in an austenitic steel weld was made in this paper. Simulated data was used, which was generated using the finite element package PZFlex. A range of simulations were created of a characterised austenitic steel weld with side drilled hole inclusions of varying radius. The DORT and TFM methods were applied to these data sets. The DORT method shows encouraging results for detection of very small inclusions and appears to outperform the TFM method for the detection of the side drilled hole of radius 0.25 mm. However the size of the inclusion cannot be determined from the images produced using the DORT method. The next stage would be to develop techniques for the characterisation of defects in steel welds which could be used along side the DORT method for detection.

February 28, 2012

References

[1] Louis Cartz. *Nondestructive Testing*. ASM International, 1999.

[2] Josef Krautkramer and Herbert Krautkramer. *Ultrasonic Testing of Materials*. Springer-Verlag, 1990.

[3] J.F. Havlice and J.C. Taenzer. Medical ultrasonic imaging: An overview of principles and instrumentation. *Proceedings of the IEEE*, 67(4):620–641, 1979.

[4] B.W. Drinkwater and P.D. Wilcox. Ultrasonic arrays for non-destructive evaluation: A review. *NDT & E Int*, 39(7):525–541, 2006.

[5] M. Fink, C. Prada, F. Wu, and D. Cassereau. Self focusing in inhomogeneous media with time reversal acoustic mirrors. In *Ultrasonics Symposium*, volume 2, pages 681 –686, 1989.

[6] C. Prada, F. Wu, and M. Fink. The iterative time reversal process: A solution to self focusing in the pulse echo mode. *JASA*, 90(2):1119–1129, 1991.

[7] C. Prada, J.L Thomas, and M. Fink. The iterative time reversal process: Analysis of the convergence. *JASA*, 97(1):62–71, 1994.

[8] C. Holmes, B.W. Drinkwater, and P.D. Wilcox. Post processing of the full matrix of ultrasonic transmit receive array data for non destructive evaluation. *NDT & E Int*, 38(8):701–711, 2005.

[9] C. Prada, S. Manneville, D. Spoliansky, and M. Fink. Decomposition of the time reversal operator: Detection and selective focusing on two scatterers. *JASA*, 99(4):2067–2076, 1996.

[10] J.G Minonzio, C. Prada, A.Aubry, and M. Fink. Multiple scattering between two elastic cylinders and invariants of the time reversal operator: Theory and experiment. *JASA*, 106(2):875–883, 2006.

[11] PZFlex Weidlinger Associates Inc. 399 West El Camino Real Mountain View CA 94040-2607.

[12] C. Nageswaran, C. Carpentier, and Y.Y. Tse. Microstructural quantification, modelling and array ultrasonics to improve the inspection of austenitic welds. *Insight*, 51(12):660–666, 2009.

[13] G. Harvey, A.Tweedie, C. Carpentier, and P. Reynolds. Finite element analysis of ultrasonic phased array inspections on anisotropic welds. In *AIP Conf. Proc.*, volume 1335, pages 827–834, 2010.

[14] D.H Chambers and A.K. Gautesen. Time reversal for a single spherical scatterer in an electromagnetic field. *JASA*, 119(7):2616–2624, 2001.

[15] A. Aubry and A.Derode. Detection and imaging in a random medium: A matrix method to overcome multiple scattering and aberration. *J. Appl. Phys.*, 106(4), 2009.

[16] Lester W.Schmerr. *Fundamentals of ultrasonic nondestructive evaluation: A modelling approach.* Plenum Press, 1998.